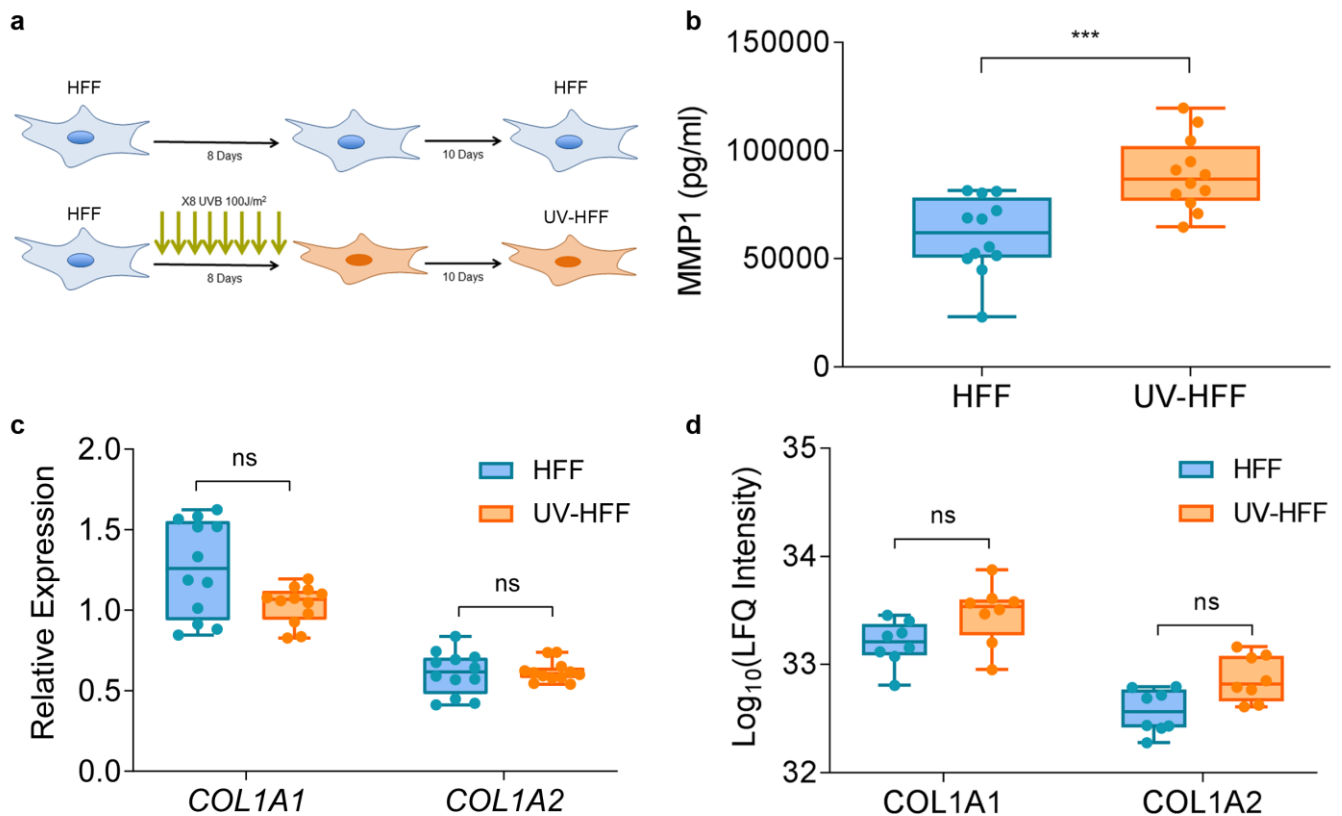
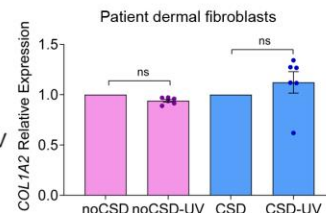
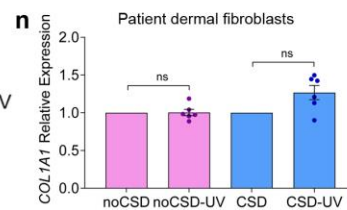
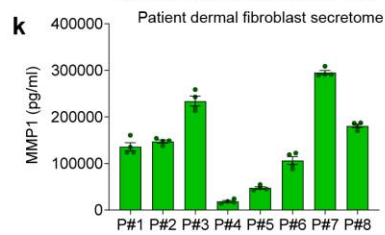
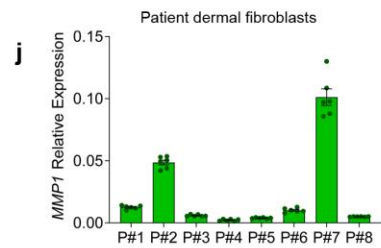
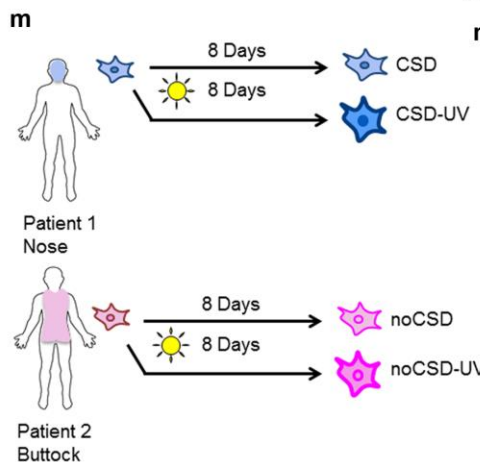
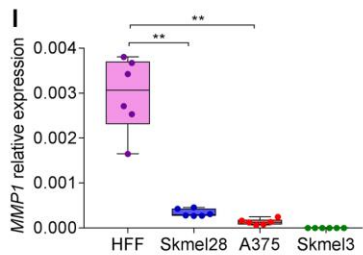
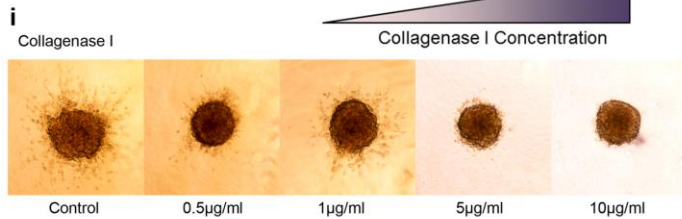
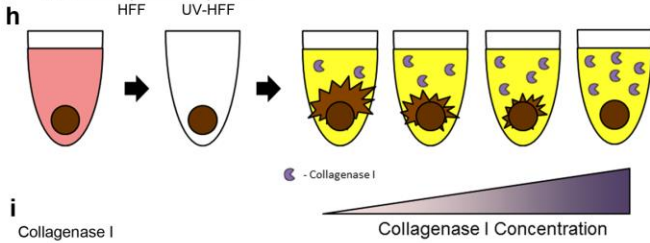
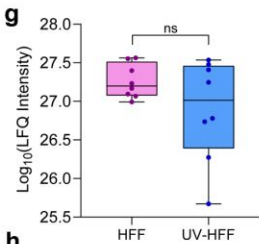
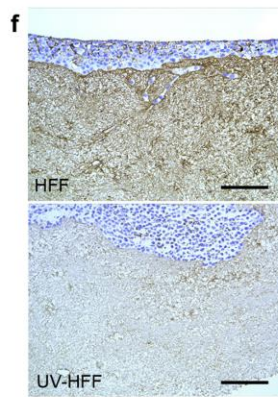
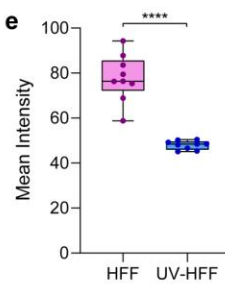
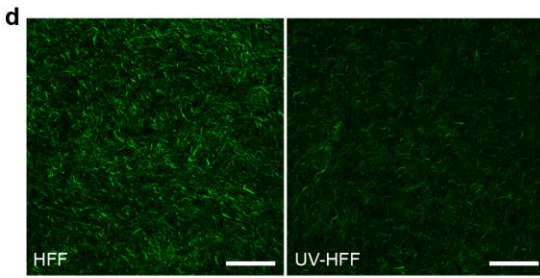
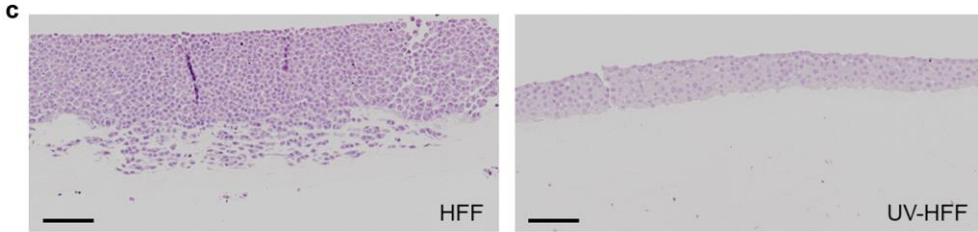
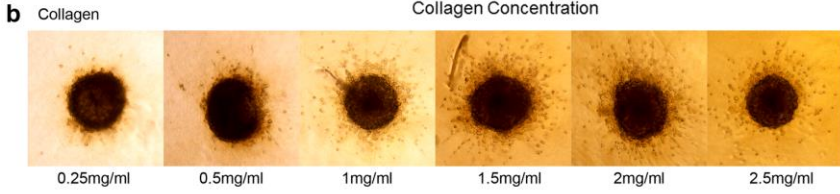
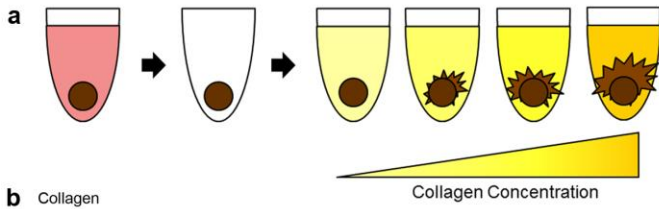


Supplementary Information

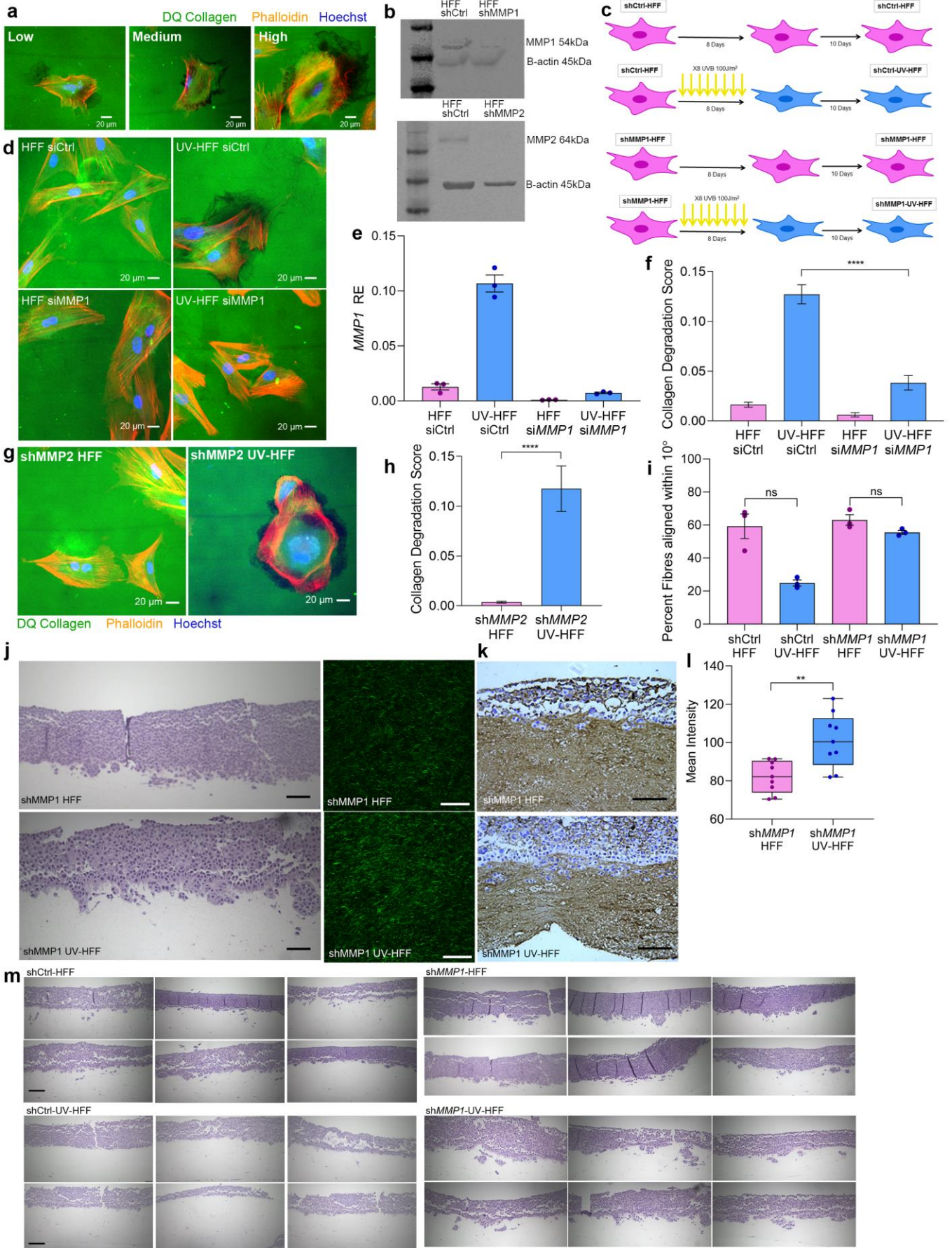


Supplementary Figure 1. UVR damaged fibroblasts upregulate MMP1 but not COL1A1. **a.** Graphic representation of the generation of isogenic HFF and UV-HFF by chronic UVR treatment. **b.** Quantification of MMP1 in the secretome of HFF and UV-HFF fibroblasts, (two-sided Mann Whitney U *** $p=0.0009$). **c.** Relative Expression of *COL1A1* and *COL1A2* in HFF and UV-HFF fibroblasts, (two-sided Mann Whitney U ns: not significant). **d.** Label free quantification (LfQ) of *COL1A1* AND *COL1A2* in the HFF and UV-HFF matrisome by mass spectrometry, (two-sided Mann Whitney U ns: not significant). All data represents duplicate samples collected from biological replicate cell lines, box plot showing biological and technical replicate points. box plots represent 25th to 75th percentiles with median, whiskers represent minimum and maximum values.



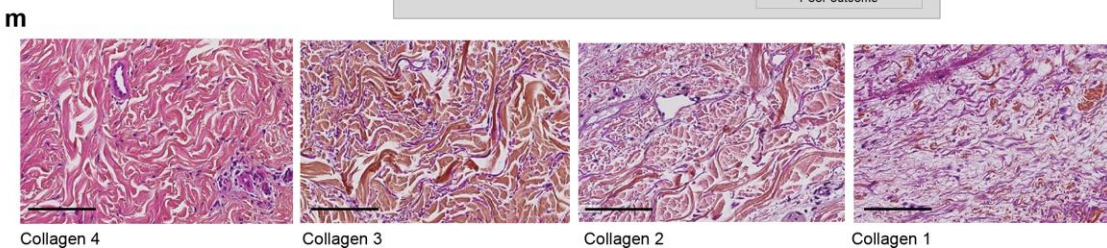
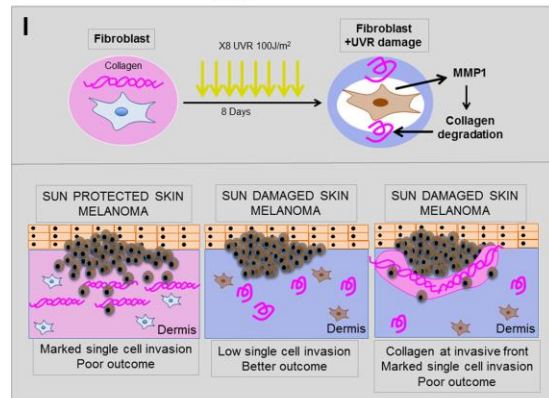
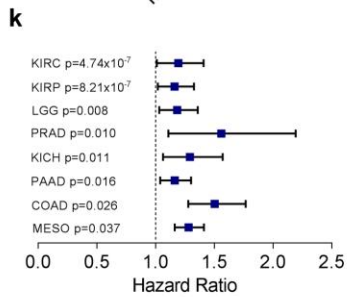
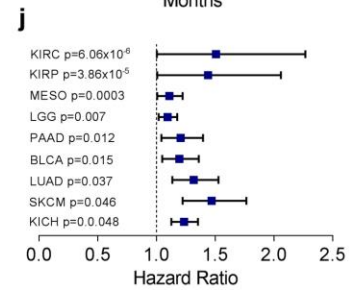
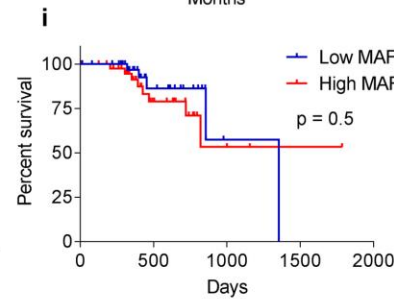
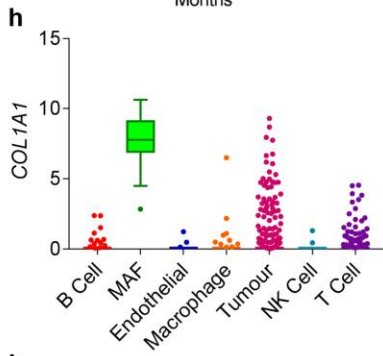
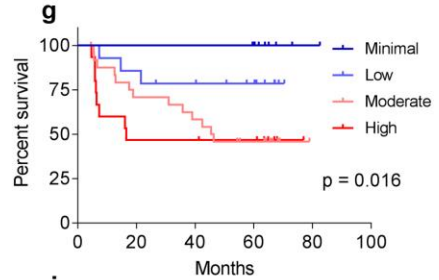
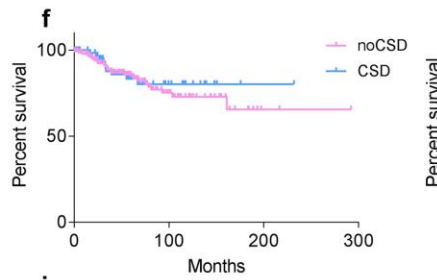
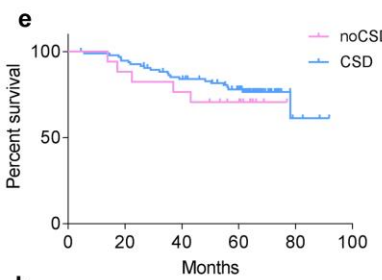
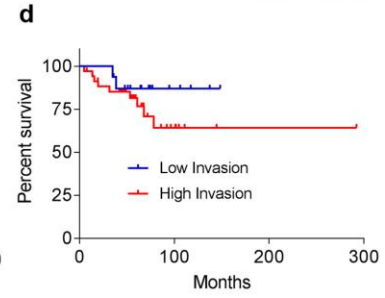
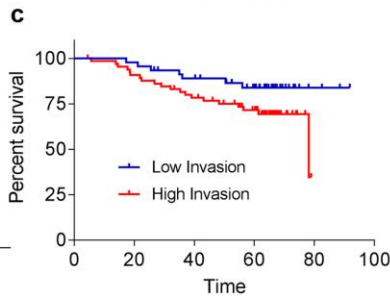
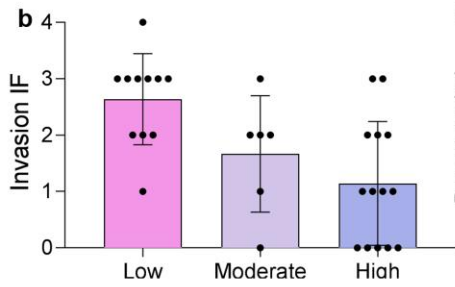
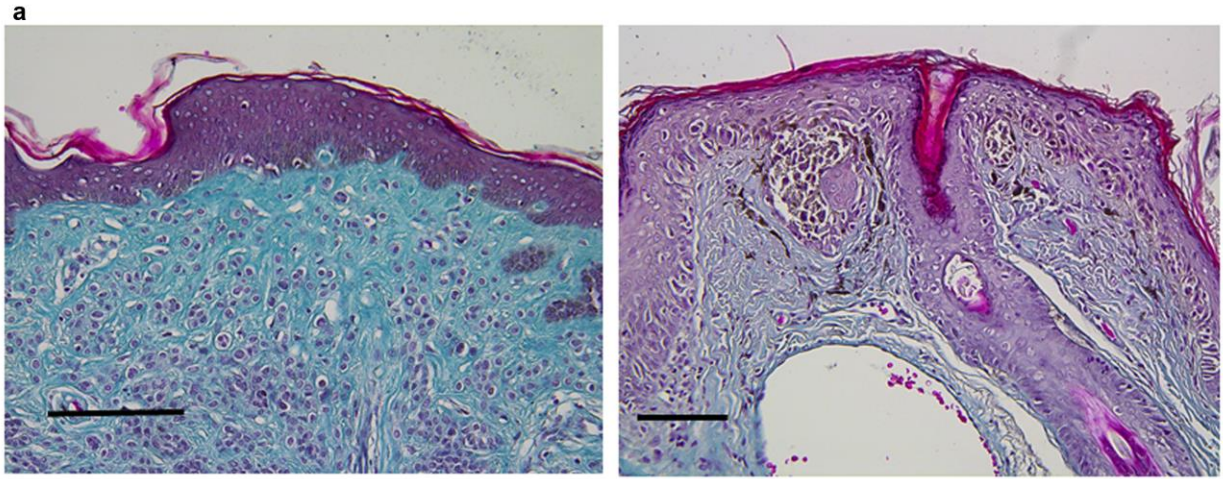
Supplementary Figure 2. Melanoma invasion decreases in low amounts and degraded collagen

a. Graphical representation of spheroid model of collagen concentration gradient. **b.** Representative Sk-mel-28 spheroid invasion in collagen gradient. **c.** Representative H&E photomicrographs of UV and UV-HFF constructs with melanoma cells, scale bar: 150 μm . **d.** Second harmonic generation (SHG) imaging of collagen fibres in organotypic dermal collagen HFF and UV-HFF constructs, scale bar: 50 μm . **e.** Quantification of collagen from SHG images in HFF and UV-HFF, (two-sided Mann Whitney U **** $p < 0.0001$). **f.** Fibronectin IHC staining in organotypic dermal collagen HFF and UV-HFF constructs, scale bars: 50 μm . **g.** Label free quantification (LFQ) of elastin (ELN) in the HFF and UV-HFF matrix by mass spectrometry (two-sided Mann Whitney U ns: not significant). **h.** Graphical representation of spheroid model of collagenase I concentration gradient. **i.** Representative Sk-mel-28 spheroid invasion in collagenase I gradient. **j.** Relative expression of *MMP1* in panel of eight healthy adult dermal fibroblasts cell lines. **k.** Quantification of *MMP1* in the secretome of eight adult fibroblast cell lines. **l.** Relative expression of *MMP1* in melanoma cell lines (Sk-mel-28, A375, Sk-mel-3) compared to HFF fibroblasts, (two-sided Mann Whitney U ** $p = 0.0022$). **m.** Graphical representation of isogenic chronic UVR model in two adult fibroblast lines. **n.** Fold change in expression of *COL1A1* and *COL1A2* in chronic UVR fibroblasts normalised to isogenic untreated cell lines, (two-sided Mann Whitney U ns: not significant). Error bars: standard error of the mean (bar). Box plots represent 25th to 75th percentiles with median, whiskers represent minimum and maximum values.



Supplementary Figure 3. UVR damage to human dermal fibroblasts upregulate MMP1 but not COL1A1

a Representative images of collagen degradation scores as outlined in methods. **b** Western blots validating knockdown of MMP1 and MMP2 in shRNA cell lines. **c** Graphical representation of isogenic chronic UVR model in shCtrl and shMMP1 HFF fibroblasts. **d** Representative images of collagen degradation in siCtrl-HFF, siCtrl-UV-HFF, siMMP1-HFF and siMMP1-UV-HFF fibroblasts. Green: intact DQ collagen; red: phalloidin; blue: Hoechst. Size bars: 20 μ m. **e** Validation of siRNA effect on MMP1 relative expression (RE) by qPCR in collagen degradation assay. **f** Quantification of collagen degradation of siCtrl-HFF and siMMP1-HFF (pink) and their isogenic chronic UVR cell lines siCtrl-UV-HFF and siMMP1-UV-HFF (blue), (two-sided Mann Whitney U **** $p < 0.0001$). **g** Representative images of collagen degradation in shMMP2-HFF, and shMMP2-UV-HFF fibroblasts. Green: intact DQ collagen; red: phalloidin; blue: Hoechst. Scale bars: 20 μ m. **h** Quantification of collagen degradation of shMMP2-HFF and their isogenic chronic UVR cell line shMMP2-UV-HFF (blue), (two-sided Mann Whitney U **** $p < 0.0001$). **i** Quantification of fibres within 10° of mode orientation in shCtrl-HFF, shCtrl-UV-HFF, shMMP1-HFF and shMMP1-UV-HFF derived ECM by fibronectin immunofluorescence (shCtrl-HFF vs shCtrl-UV-HFF $p = 0.1$ ($n = 3$), ns: not significant) **j** Representative H&E images of shMMP1-HFF and shMMP1-UV-HFF fibroblasts, scale bars: 75 μ m (left) and second harmonic generation (SHG) imaging of collagen fibres in organotypic dermal collagen shMMP1-HFF and shMMP1-UV-HFF constructs (right), scale bars: 50 μ m. **k** Fibronectin IHC staining in organotypic dermal collagen shMMP1-HFF and shMMP1-UV-HFF constructs, scale bars: 50 μ m. **l** Quantification of collagen from SGH images in shMMP1-HFF and shMMP1-UV-HFF (two-sided Mann Whitney U, ** $p = 0.004$). **m** Representatives H&E photomicrographs of shCtrl-HFF (four top left images), shCtrl-UV-HFF (four top right images), shMMP1-HFF (four bottom left images) and shMMP1-UV-HFF (four bottom right images) derived ECM constructs with invading melanoma cells, scale bars: 100 μ m, scale for all images equal. Error bars: standard error of the mean (bar). Box plots represent 25th to 75th percentiles with median, whiskers represent minimum and maximum values.



Collagen 4

Collagen 3

Collagen 2

Collagen 1

Supplementary Figure 4. Collagen at the invasive front or primary invasive cutaneous melanoma drives melanoma invasion and poor outcome

a Trichrome of Masson stain (blue) of collagen in sun protected skin (left, scale bar 200 μm) and sun damaged skin (right, scale bar 200 μm). **b** Correlation between ECM degradation of the adjacent dermis and invasive score of melanoma tumour cells at the invasive front (IF) in the A cohort. **c** Kaplan-Meier of melanoma specific survival (MSS) in prominent (high, red) and minimal (low, blue) melanoma invasion at the IF (C cohort, n=112). **d** Kaplan-Meier of melanoma specific survival (MSS) in prominent (high, red) and minimal (low, blue) melanoma invasion at the IF (B cohort, n=51). **e** Kaplan-Meier of MSS in melanoma invading in chronic sun damaged (CSD, blue) and no chronic sun damage (noCSD, pink) dermis (C cohort, n=113). **f** Kaplan-Meier of MSS in melanoma invading in CSD (blue) and noCSD (pink) dermis (B cohort, n=216). **g** Kaplan-Meier of progression free survival by collagen quantity at the IF (two-sided Log Rank test, C cohort, n=63). **h** *COL1A1* expression by cell type in metastatic melanoma single cell RNA-seq (MAF: melanoma associated fibroblast, NK cell: natural killer cell, Tirosh *et al.* Science 2016). **i** Kaplan-Meier of MSS by melanoma associated fibroblast (MAF) signature score without collagen genes in aged (>54) primary cutaneous melanoma cohort (two-sided Log Rank test, TCGA cohort, n=80). **j** Hazard ratio (centre) and 95% CI (bars) for OS, and PFS **k** Univariate Cox regression of *COL1A1* expression by cancer type in PANCAN TCGA in aged population (≥ 55 years) (BLCA, Bladder urothelial carcinoma, COAD, Colon adenocarcinoma, KICH, Kidney chromophobe, KIRC, Kidney renal clear cell carcinoma, KIRP, Kidney renal papillary cell carcinoma, LGG, Brain lower grade glioma, LUAD, Lung adenocarcinoma, MESO, Mesothelioma, PAAD, Pancreatic adenocarcinoma PRAD, Prostate adenocarcinoma, SKCM, Skin Cutaneous Melanoma). **l** Graphic summary of study. Risk tables for all Kaplan-Meier analyses in Supplementary Data 2. Error bars: standard error of the mean (bar). **m** Representative photomicrographs of collagen scoring. 4: preservation of collagen fibres in the dermis. 3. Combination of preserved, normal collagen bundles (pink) intermixed with elastotic fibres of non-collagenous material (purple). 2. Combination of some collagen (pink) with purple elastotic fibres. Multiple fragmentation of collagen. 1. Scarce or absent collagen, substitution of the matrix by elastotic heterogeneous fibres (purple). Rare collagen fragments interspersed (pink). Scale bars: 100 μm .

Gene Set Name	# Genes in Gene Set (K)	Description	# Genes in Overlap (k)	k/K	p-value	FDR q-value
REACTOME_EXTRACELLULAR_MATRIX_ORGANIZATION	301	Extracellular matrix organization	48	0.1595	1.91E-27	2.86E-24
REACTOME_COLLAGEN_FORMATION	90	Collagen formation	25	0.2778	4.28E-21	3.21E-18
REACTOME_DEVELOPMENTAL_BIOLOGY	1104	Developmental Biology	73	0.0661	2.54E-17	1.27E-14
REACTOME_HEMOSTASIS	674	Hemostasis	54	0.0801	1.59E-16	5.96E-14
REACTOME_ASSEMBLY_OF_COLLAGEN_FIBRILS_AND_OTHER_MULTIMERIC_STRUCTURES	61	Assembly of collagen fibrils and other multimeric structures	18	0.2951	4.32E-16	1.29E-13
REACTOME_AXON_GUIDANCE	554	Axon guidance	47	0.0848	1.79E-15	4.47E-13
REACTOME_COLLAGEN_BIOSYNTHESIS_AND_MODIFYING_ENZYMES	67	Collagen biosynthesis and modifying enzymes	18	0.2687	2.73E-15	5.85E-13
REACTOME_CELL_JUNCTION_ORGANIZATION	92	Cell junction organization	20	0.2174	6.74E-15	1.26E-12
REACTOME_CELL_CELL_COMMUNICATION	130	Cell-Cell communication	22	0.1692	7.41E-14	1.23E-11
REACTOME_INTEGRIN_CELL_SURFACE_INTERACTIONS	85	Integrin cell surface interactions	18	0.2118	2.45E-13	3.68E-11

Supplementary Table 1. Top 10 Reactome pathways significantly enriched by genes differentially expressed by Signature 7 mutation count

ID	Gene	Expression Change
COL3A1	collagen type III alpha 1 chain	DOWN
COL5A1	collagen type V alpha 1 chain	DOWN
COL5A3	collagen type V alpha 3 chain	DOWN
COL4A1	collagen type IV alpha 1 chain	DOWN
COL4A2	collagen type IV alpha 2 chain	DOWN
COL1A1	collagen type I alpha 1 chain	DOWN
ITGA6	integrin subunit alpha 6	DOWN
COL10A1	collagen type X alpha 1 chain	DOWN
COL8A1	collagen type VIII alpha 1 chain	DOWN
COL8A2	collagen type VIII alpha 2 chain	DOWN
COL11A1	collagen type XI alpha 1 chain	DOWN
COL15A1	collagen type XV alpha 1 chain	DOWN
PLEC	plectin	DOWN
CD151	CD151 molecule (Raph blood group)	DOWN
MMP3	matrix metalloproteinase 3	UP
CTSL	cathepsin L	UP
LOX	lysyl oxidase	DOWN
LOXL2	lysyl oxidase like 2	DOWN
COL26A1	collagen type XXVI alpha 1 chain	DOWN
P4HB	prolyl 4-hydroxylase subunit beta	DOWN
SERPINH1	serpin family H member 1	DOWN
COLGALT2	collagen beta(1-O)galactosyltransferase 2	DOWN
PLOD1	procollagen-lysine,2-oxoglutarate 5-dioxygenase 1	DOWN
P3H2	prolyl 3-hydroxylase 2	DOWN
COLGALT1	collagen beta(1-O)galactosyltransferase 1	DOWN
ITGB1	integrin subunit beta 1	DOWN
DAG1	dystroglycan 1	DOWN
ACTN1	actinin alpha 1	DOWN
FN1	fibronectin 1	DOWN
ITGB2	integrin subunit beta 2	DOWN
MMP1	matrix metalloproteinase 1	UP
SPARC	secreted protein acidic and cysteine rich	DOWN
APP	amyloid beta precursor protein	UP
HSPG2	heparan sulfate proteoglycan 2	DOWN
COMP	cartilage oligomeric matrix protein	DOWN
ICAM2	intercellular adhesion molecule 2	DOWN
ICAM5	intercellular adhesion molecule 5	DOWN
ITGA11	integrin subunit alpha 11	DOWN
MMP8	matrix metalloproteinase 8	UP
DCN	decorin	UP
ELN	elastin	DOWN
SCUBE3	signal peptide, CUB domain and EGF like domain containing 3	DOWN
BGN	biglycan	DOWN
ASPN	asporin	DOWN
BMP2	bone morphogenetic protein 2	UP
EFEMP2	EGF containing fibulin extracellular matrix protein 2	DOWN
BMP7	bone morphogenetic protein 7	UP
MFAP5	microfibril associated protein 5	DOWN

Supplementary Table 2. Genes from Reactome Extracellular Matrix Organisation pathway differentially expressed by Signature 7 mutations

Age median (range)	69	(34-75)
Sex	6 Female	2 Male
Anatomic site	7 Limbs and trunk	1 Head and neck

Supplementary Table 3. Patient fibroblasts

Variable	Cohort A		Cohort B		Cohort C	
	(N=31)		(N=222)		(N=113)	
Age - median \pm SD (range)	68.84 \pm 7.87	(57-91)	69.5 \pm 9.15	(55-96)	67 \pm 8.86	(55 - 88)
Sex						
Male (%)	NA		140	(63.06)	63	(55.75)
Female (%)	NA		82	(36.94)	50	(44.25)
Breslow - median \pm SD (range)	1.72 \pm 2.74	(0.1-14)	2.2 \pm 2.20	(1-13.5)	2.5 \pm 3.91	(1 - 35)
Site						
Trunk (%)	NA		74	(33.33)	53	(46.90)
Head&neck (%)	NA		86	(38.74)	13	(11.50)
Upper limb (%)	NA		26	(11.71)	19	(16.81)
Lower limb (%)	NA		36	(16.22)	28	(24.79)
Solar elastosis						
noCSD (%)	17	(54.8)	149	(67.12)	17	(15.04)
CSD (%)	14	(45.2)	73	(32.88)	96	(82.22)

Supplementary Table 4. Clinical cohort details

Variable	Cox regression model											
	Univariate			Multivariate (a)			Multivariate (b)			Multivariate (c)		
	HR	95% CI	P-value	HR	95% CI	P-value	HR	95% CI	P-value	HR	95% CI	P-value
Age	1.03	1.00-1.06	0.03*	1.02	0.95-1.05	0.47	1.02	0.98-1.05	0.4	1.02	0.97-1.08	0.4
Sex												
Female	ref	ref	ref	ref	ref	ref	ref	ref	ref	ref	ref	ref
Male	2.04	1.18-3.55	0.01*	1.43	0.48-3.77	0.49	2.67	1.22-5.88	0.01*	1.3	0.48-3.48	0.6
Breslow	1.06	1.03-1.10	0.0004*	1.03	0.87-1.33	0.77	1.09	1.04-1.15	0.0009*	1	0.85-1.20	0.9
CSD												
noCSD	ref	ref	ref	ref	ref	ref	-	-	-	-	-	-
CSD	0.99	0.61-1.65	0.36	0.73	0.16-1.57	0.57						
Invasion Binary												
Low	ref	ref	ref	ref	ref	ref	ref	ref	ref	-	-	-
High	2.3	1.09-4.85	0.03*	1.17	0.39-5.41	0.81	2.76	1.21-6.27	0.02*			
Invasive Front Collagen	1.9	1.15-3.15	0.01*	1.7	1.00-3.13	0.06	-	-	-	1.85	1.11-3.1	0.019*

(a) multivariate analysis with all variables

(b) multivariate analysis with clinical variables significant in univariate and invasion score

(c) multivariate analysis with clinical variables significant in univariate and collagen scores

*p<0.05

Supplementary Table 5. Cox regression of clinical and invasion variables